Chemical composition of size-resolved atmospheric aerosols in the eastern Mediterranean during summer and winter

H. Bardouki[a], H. Liakakou[a], C. Economou[a], J. Sciare[b], J. Smolík[c], V. Ždímal[c], K. Eleftheriadis[d], M. Lazaridis[e], C. Dye[f], N. Mihalopoulos[a],*

[a] *Environmental Chemical Processes Laboratory, Department of Chemistry, University of Crete, P.O. Box 1470, 71409 Heraklion, Greece*
[b] *LSCE, Orme des Merisiers, Bat 709, CE Saclay, 91191 Gif-sur-Yvette Cedex, France*
[c] *Institute of Chemical Process Fundamentals AS CR, Prague, Czech Republic*
[d] *Institute of Nuclear Technology—Radiation Protection, N.C.S.R. ''Demokritos'', Athens, Greece*
[e] *Technical University of Crete, Chania, Greece*
[f] *NILU, PO Box 100, N 2007 Kjeller, Norway*

Abstract

The chemical composition of aerosols has been determined in 30 size-resolved samples collected using a Berner low-pressure impactor during two campaigns conducted at a coastal site in the Eastern Mediterranean in July 2000 and in January 2001. Sulfate (SO_4^{2-}) and ammonium (NH_4^+) have been identified as the main ionic components of the sub-micronic aerosol fraction, with SO_4^{2-} accounting for up to 38% of the total fine mass and up to 65% of the total ionic mass during both seasons. On the other hand, nitrate (NO_3^-), chloride (Cl^-), sodium (Na^+) and calcium (Ca^{2+}) were identified as the main components of the super-micron mode. The ionic organic compounds (including carboxylic, dicarboxylic and ketoacids) were distributed both between sub-micron and super-micron mode, indicating origin from both gas-to-particle conversion and heterogeneous reactions on pre-existing particles. The total water-soluble ionic organic fraction although accounting for only up to 1–2% of both coarse ($> 1\,\mu m$) and fine ($< 1\,\mu m$) mass fractions, accounts for up to 15% of the organic carbon (OC) mass.

NH_4^+ was found to be significantly correlated to non-sea-salt sulfate (nss-SO_4^{2-}), with NH_4^+/nss-SO_4^{2-} molar ratio ranging from 1.3 to 2, the lower ratio associated with transport from the W sector. Chloride depletion was observed mainly during summer and was significantly correlated with NO_3^- concentrations, with a molar ratio of 0.80, indicating the reaction of nitric acid with NaCl as the main source of NO_3^- in the area.

Total ionic mass both in the fine and coarse fraction accounted for up to 58% of the total aerosol mass during both seasons. An attempt to perform a mass closure analysis indicates that nss-SO_4^{2-} and organic carbon are the main components of the fine fraction with relative contributions of 38% and 16%, respectively. In the coarse fraction, the ionic part accounts for 58%, mineral dust for 32% and the remaining non-identified part of 12–30% could be partly attributed to water.

© 2002 Elsevier Science Ltd. All rights reserved.

Keywords: Size resolved aerosol composition; Regional pollution; Eastern Mediterranean

1. Introduction

Atmospheric aerosols affect the Earth's climate both directly through scattering and absorption of solar radiation and indirectly acting as cloud condensation

---

*Corresponding author. Tel.: +30-810-393-662; fax: +30-810-393-601.

E-mail address: mihalo@chemistry.uoc.gr (N. Mihalopoulos).

nuclei (CCN). A 2% increase in aerosol planetary albedo is sufficient to compensate global warming due to doubling of greenhouse gas emissions (IPCC, 2001). The largest uncertainties in the estimation of direct and indirect radiative forcing from aerosols are related to the insufficient knowledge of the high spatial and temporal variability of aerosol concentrations, of their micro-physical, chemical and radiative properties (IPCC, 2001). Therefore, there is an urgent need for undertaking a systematic study and appraisal of physical and chemical properties of the atmospheric aerosol.

Model estimations (Charlson et al., 1991) as well as measurements (Ichoku et al., 1999; Andreae et al., 2002) show very important radiative forcing induced by aerosols above the Eastern Mediterranean. The Eastern Mediterranean area can be affected by three strong, but very different in composition, aerosol sources: Sahara desert, industrialized areas of N/NE Europe and sea-spray (Mihalopoulos et al., 1997; Moulin et al., 1997a, b; Kubilay et al., 2000; Ganor and Mamane, 1982).

To investigate the chemical composition (with em-phasis on the ionic part) of aerosol, size-segregated samples have been collected at a coastal rural site on the island of Crete, in the Eastern Mediterranean using low pressure 10 stages cascade impactors during two seasons (summer and winter).

Size-segregated ionic composition measurements have been performed to provide information on the sources and the formation pathways of specific compounds. The total mass has been also measured at each stage and compared with the corresponding total ionic mass.

Special attention is paid on the size distribution of carboxylic, dicarboxylic and ketoacids. These com-pounds are ubiquitous chemical constituents of the troposphere, an important group of the water-soluble organics, contribute to both the acidity of precipitation and to the particulate organic carbon budget and could act as condensation nuclei (CN) and cloud condensation nuclei (CCN; Kawamura and Usukura, 1993; Chebbi and Carlier, 1996; Matsumoto et al., 1997; Yu, 2000). For instance, Matsumoto et al. (1997) found a significant correlation between total water soluble organic salt (formate, acetate, oxalate and methanesul-fonate) concentrations and CCN concentrations at 1% and 0.5% super-saturation. Note that data on size distribution of carboxylic, dicarboxylic and ketoacids are sparse in the literature and completely missing for the Mediterranean area.

2. Experimental

2.1. Sampling

During the periods of 10–31 July 2000 and 7–14 January 2001 size-segregated samples were collected at Finokalia ($35°19'$N, $25°40'$E) on Crete Island using Berner type low-pressure cascade impactor (BLPI 25/ 0.018/2). Details about the Finokalia sampling station and the meteorological prevailing conditions can be found elsewhere (Mihalopoulos et al., 1997; Kouvarakis et al., 2000).

Sampling was carried out at the top of a small building $\sim$150 m a.s.l. facing the sea within the sector of $270–90°$. The impactor had an inlet providing approxi-mately 15 μm upper cut-off particle size and operated at a flow rate of $25\,l\,min^{-1}$. As calibrated at the Finnish Meteorological Institute by the method described by Hillamo and Kaupinnen (1991), the impactor separated the particles into the following aerodynamic equivalent diameter (Dp) ranges: 6.8; 3.39; 1.72; 0.85; 0.44; 0.25; 0.17; 0.11; 0.06 and 0.024 μm. To reduce particle bounce, Nuclepore polycarbonate foils greased with Apiezon L vacuum grease were used. Sampling was carried out approximately in 24 h intervals (starting at 10:00 during summer and at 14:00 during winter). Time is expressed as local time (LT = UTC + 3 h during summer).

2.2. Analysis

Following collection, the foils were transported from the sampling site in Petri dishes and equilibrated in the weighting room for at least 24 h before weighing. A quarter of the foil was dedicated to ion chromatography analysis. This part was kept refrigerated until analysis and was extracted by sonication for 45 min in 15 ml of ultra-pure water. The extraction efficiency of this method is higher than 98% for all compounds of interest. Chloroform of 100–200 μl was added as a biocide in the sample extracts which were analyzed within a week after extraction.

A Dionex AS4A-SC column with ASRS-I suppressor in auto-suppression mode of operation was used for the analysis of anions (chloride: Cl^-, bromide: Br^-, nitrate: NO_3^-, sulfate: SO_4^{2-}, oxalate: $C_2O_4^{2-}$ and methanesulfo-nate: MS^- ($CH_3SO_3^-$)). All the anions, except MS^- were determined with isocratic elution at $2.0\,ml\,min^{-1}$ of $Na_2CO_3/NaHCO_3$ eluent. The light carboxylic, dicar-boxylic, ketoacids and MS^- were analyzed using a Dionex DX-500 ion chromatography with an AS11 analytical column and NaOH (0.1–3.5 mM) as eluent in a gradient mode. Under the experimental conditions, which were similar to that used by Kerminen et al. (1999) and Jaffrezo et al. (1998), a very good separation was achieved between the organic acids except for malonate that in some cases was not well resolved from the carbonate peak. For that reason no malonate concentrations are reported here. For the cations (sodium: Na^+, ammonium: NH_4^+, potassium: K^+, magnesium: Mg^{2+} and calcium: Ca^{2+}) a CS12-SC column was used with a CSRS-I suppressor. Separation

was achieved under isocratic conditions with 20 mM MSA eluent and flow rate of 1.0 ml min^{-1}. The reproducibility of the measurements was better than 2% and the detection limit ranged from around 1 ppbv for the main anions and cations to below 0.1 ppbv for the main organic ions and MS$^-$ (1 ppbv corresponds to 0.37 ng m^{-3} for a mean air volume of 40 m^3). Mean blank values were 5–10 ppbv for Na$^+$, Ca^{2+}, and lower than 3 pbbv for the rest of the main anions and cations, 5–10 ppbv for acetate and formate, 1 ppbv for MS$^-$, 0.5 ppbv for pyruvate and oxalate and below the detection limits for the rest of the organic ions. Stage concentrations were corrected for blanks resulting sometimes in negative values (less than 15% of the cases and mainly for the organic ions acetate, formate and pyruvate). In that case the negative values were replaced by zero. More details on the analytical technique are given by Baboukas et al. (2000) and Kouvarakis and Mihalopoulos (2002).

- ^{222}Rn was used during the campaign as a continental tracer. ^{222}Rn is a noble gas injected in the troposphere mainly from the continents and disappears only through radioactive decay with a half-lifetime of 3.8 days. ^{222}Rn activities were estimated through collection of its short-lived decay aerosol products on cellulose filters and consequently detection of their radioactivity by an alpha scintillation counter. Sampling step was 2 h with detection limit of 0.01 pCi m^{-3}. Details on ^{222}Rn measurements and its use as a continental tracer are reported by Polian et al. (1986).
- Back-trajectory calculations were made using the HYSPLIT_4 (Hybrid Single-Particle Langrangian Integrated Trajectory) modeling system. This public domain model (http://www.arl.noaa.gov/ready/hys-plit4.html) is documented in the international literature (Draxler and Hess, 1998). The meteorological data used in the calculations were obtained from the National Weather Service's of the National Centre for Environmental Prediction (NCEP) of USA.

3. Results and discussion

3.1. Chemical composition

3.1.1. Variation of the main ionic species (total concentrations)

Table 1 presents the mean variation of the main ionic species, during the whole experiment and for each season.

Examination of these data leads to the following conclusions:

- For the main anions, cations and MS$^-$, the reported concentrations are in a very good agreement with the

Table 1

Levels (mean and standard deviation) of the main ionic and organic ionic species, determined during the whole experiment and for both seasons

Species	Concentration (ng m^{-3})			
	Summer		Winter	
	Mean	SD	Mean	SD
Ca^{2+}	1510.1	198.2	156.6	26.3
Mg^{2+}	303.9	44.7	207.6	29.2
K$^+$	294.0	34.0	163.0	17.1
NH$_4^+$	2370.9	379.1	770.6	85.6
Na$^+$	2027.9	280.8	1199.0	183.8
SO$_4^{2-}$	6877.1	958.0	2363.0	385.1
NO$_3^-$	2750.4	415.0	1528.0	226.5
Cl$^-$	2278.5	360.1	2056.9	300.9
MS$^-$	32.1	3.6	17.0	1.1
HCOO$^-$	135.7	3.9		
CH$_3$COO$^-$	114.7	4.2		
C$_3$H$_5$O$_2^-$	17.9	1.1		
C$_2$O$_4^{2-}$	255.3	19.7	68.6	5.4
C$_4$H$_4$O$_4^{2-}$	3.7	0.2	3.3	0.1
C$_5$H$_6$O$_4^{2-}$	1.8	0.1	2.5	0.3
C$_3$H$_3$O$_3^-$	23.1	1.2	11.1	0.7

results at Finokalia reported by Mihalopoulos et al. (1997) and Kouvarakis and Mihalopoulos (2002) during summer and winter, as well as with the values reported for these compounds in other parts of the Mediterranean (Sellegri et al., 2001; Andreae et al., 2002 and references therein).

- For the carboxylic (formate, acetate and propionate), dicarboxylic (oxalate, succinate and glutarate) and ketocarboxylic anions (pyruvate), the above reported results are, to our knowledge, the first reported for the southern Europe. The above measured organic species account for the majority (more than 80%) of the organic acids existing in the aerosol phase (Kawamura et al., 1996; Kawamura and Sakaguchi, 1999; Krivácsy et al., 2001).

Table 2 compares the levels of the organic acids measured during this work with the literature. Table 2 also presents results on aerosol phase dicarboxylic acids obtained during the period of 25–29 July 2000 aboard of the research vessel "AEGAIO" cruising the Aegean Sea along selected tracks calculated by forward and back trajectory modeling with the Finokalia sampling site as the end point. More details about the track of the vessel and the measurements performed on-board will be reported elsewhere (Eleftheriadis et al., unpublished data). For the monocarboxylic acids, the measured levels are in good agreement with those reported in the

Table 2
Aerosol concentrations (in ng m^{-3}) of acetate, formate, pyruvate, oxalate, succinate and glutarate observed during this work and comparison with other studies

Location	Acetate	Formate	Pyruvate	Oxalate	Succinate	Glutarate	Ref.
Barrow, Alaska	41	20.2	3.6	25.2			Li and Winchester (1989)
Canada Alert			<0.003–0.52	1.8–70	0.51–18	0.16–4.3	Kawamura et al. (1996)
Finland (Arctic)				6–55	7–48	3–23	Kerminen et al. (1999)
Dayllbagh, India	319[a]	156[a]					Khare et al. (1998)
K-Puszta		91		269	5		Krivácsy et al. (2001)
Mace-Head		13		48	<2		
Finokalia				336.1[c]	8.2[c]	3.3[c]	This work
(summer)	114.7	135.7	23.1	255.3	3.7	1.8	This work
(winter)			11.1	68.6	3.3	2.5	This work
Pacific (34°N–14°S)				6.5–161	0.29–16	<0.01–6.3	Kawamura and Sakaguchi (1999)
NW Pacific	42.7	117		89.4			Matsumoto et al. (1998)
Atlantic	168[b]	59.8[a]	10.3	46.4			Baboukas et al. (2000)
NW Atlantic		60.7	10.0				Andreae et al. (1987)

[a] Summer values.
[b] Fine fraction.
[c] Collected on board of a ship (25–30 July 2001).

literature as well as with the long-term levels of these acids measured at Finokalia (Kouvarakis and Mihalopoulos, unpublished data). The levels of pyruvate measured at Finokalia during winter are comparable to those reported for the Atlantic Ocean (Andreae et al., 1987; Baboukas et al., 2000). On the other hand, during summer the levels of pyruvate are more than twice as high as others quoted in Table 2, denoting a significant contribution from both natural and anthropogenic sources. The levels of oxalate, especially those reported during summer as well as those observed during the cruise above the Aegean sea (336 ng m^{-3}) are among the highest reported in the literature for rural areas (Table 2). Apart from the production of oxalic acid from natural (seawater) and anthropogenic sources (photo-oxidation of olefins by O_3), oxalate is considered as the end-product of the photo-chemical breakdown of the higher dicarboxylic acids and unsaturated fatty acids after reaction with O_3 (Kawamura and Sakaguchi, 1999). The high insolation and the high levels of O_3 (up to 87 ppbv) prevailing during summer in the area could account for the very high concentrations of oxalate. Production of oxalate from photo-chemical breakdown of the higher dicarboxylic acids could also account for the relatively low summertime levels of succinate and glutarate and especially their low summer/

winter amplitude compared to that observed for oxalate (Table 2).

3.1.2. Factors controlling the variation of the main ionic species

Based on 5-day back trajectory analysis it was found that during the campaign, flow from the North sector associated with strong winds was the most frequent pattern with 2 exceptions: the first during the period 14–18 July mainly characterized by a western flow (marine air masses, with a small interruption with N winds on 15 July) and the second one from 28 July to the end of the month with low wind speed and thus increased local influence. Such a N/NE flow pattern is common in Crete during summer as mentioned by Mihalopoulos et al. (1997) from the results of a 5-yr back trajectories study performed at Finokalia Station. This change in air mass origin is clearly illustrated in Fig. 1A presenting the variation of non-sea-salt sulfate (nss-SO_4^{2-}) and Radon 222 (^{222}Rn) measurements performed at Finokalia during the summer campaign. ^{222}Rn presents quite high activities (up to 80 pCi m^{-3}) during the whole campaign with the exception of the period between 14 and 18 July when the air masses originate from the western sector (marine sector; mean value of 23.8 pCi m^{-3}). Nss-SO_4^{2-} is following quite well the ^{222}Rn variation ($r^2 =$
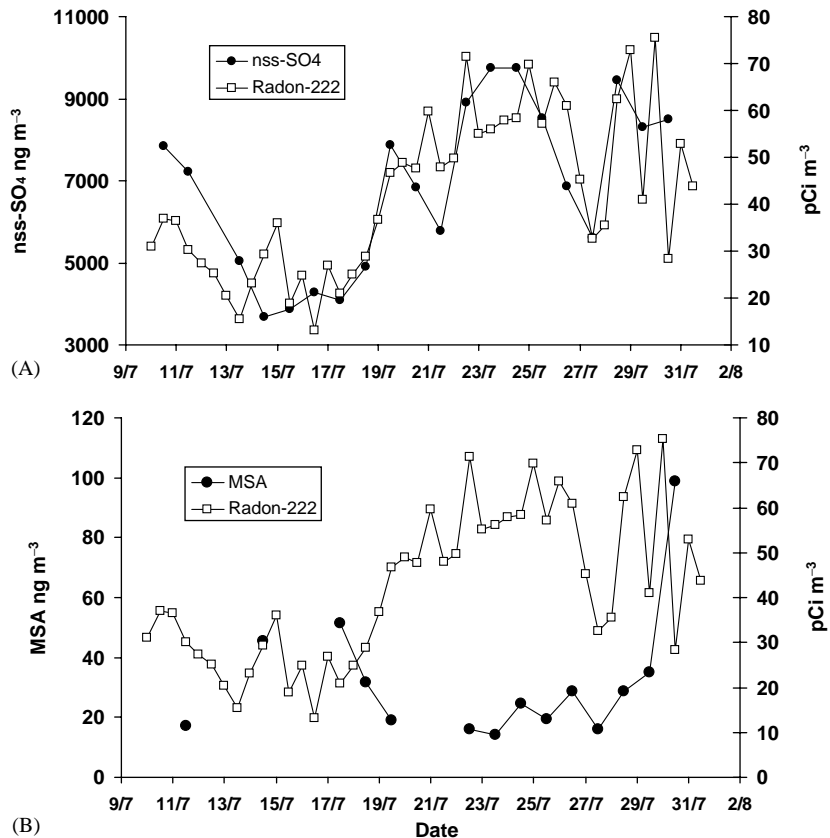
Fig. 1. Variation of nss-SO_4^{2-} and MS^- as a function of Radon 222 (^{222}Rn) activities during the summer campaign.

0.63, $P < 0.05$) indicating a major continental origin for this ion. Similar patterns with ^{222}Rn are observed both for NH_4^+ and oxalate (not shown). On the other hand MS^-, which is a product of the atmospheric oxidation of the gaseous dimethylsulfide (DMS; CH_3SCH_3) produced in seawater, presents a totally different variation with the highest values in 14, 18 and 30 July (Fig. 1B), i.e. the period with the smallest continental influence.

3.1.3. Interspecies correlation

Several statistically significant ($P < 0.05$, where P is the level of significance at $\alpha = 0.05$) interspecies correlations have been observed during this experiment and are discussed below:

- Between Mg^{2+} and Na^+ (Fig. 2A) and Cl^- and Na^+ (Fig. 2B): the relation between Na^+ and Mg^{2+} indicates that both compounds mainly originate from seawater since the slope of their regression (0.13) is close to that reported for seawater (mass ratio of 0.12). The same slope is observed for both summer and winter campaigns. The relationship between Na^+ and Cl^-, presents two different slopes during the summer (Cl/Na ratio of 1.16, $r^2 = 0.94$)

and winter (1.76, $r^2 = 0.97$), respectively. When compared to the seawater ratio of 1.8, the above slopes indicate significant Cl^- depletion during summer.

- Statistically significant relationships ($P < 0.05$) indicating common origin are also observed between acetate and formate ($r^2 = 0.9$) and methanesulfonate and pyruvate ($r^2 = 0.8$; when 1 point is excluded). The relationship between methanesulfonate and pyruvate could indicate production of pyruvate from marine biogenic sources via photo-oxidation of biogenic compounds emitted from seawater. No significant relationship is observed either between the dicarboxylic acids or between the different carboxylic, keto-carboxylic and dicarboxylic acids, indicating significant differences both in production and/or destruction pathways in agreement with the results presented by Kerminen et al. (1999).

3.1.4. Particle size distributions

Figs. 3a–h present the particle size distribution of the main anions, cations, MS^-, oxalate, acetate, formate, pyruvate and succinate during summer. In agreement
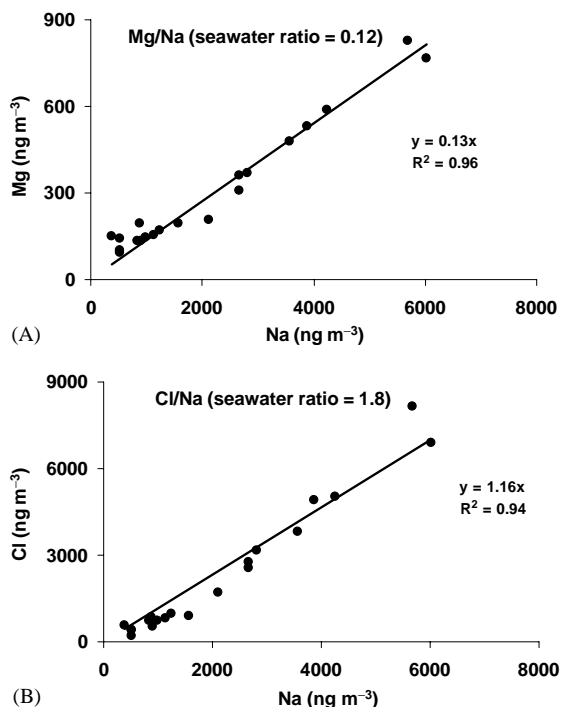
Fig. 2. Correlation between (A) Na^+ and Mg^{2+} and (B) Na^+ and Cl^- during the summer campaign.

with most aerosol size distributions reported in the literature, nss-SO_4^{2-} and NH_4^+ present their maximum in the fine mode (0.25–0.44 μm; Fig. 3a and b). In most cases, these two compounds found on the same impactor stage as shown by the statistically significant correlation coefficient (r^2 higher than 0.9; $P<0.05$) calculated for each sample using the 10 impactor stages. The NH_4^+/nss-SO_4^{2-} molar ratio ranges from 1.3 to 2, the lower ratio associated with transport from the W sector in agreement with previous observations (Quinn et al., 2000; Sellegri et al., 2001).

On the other hand, Na^+, Cl^-, K^+, Mg^{2+}, Ca^{2+} and NO_3^- present their maximum exclusively in the coarse mode (1.79–3.32 μm; Fig. 3a and b). The above pattern is expected for the five first elements (Na^+, Cl^-, K^+, Mg^{2+}, Ca^{2+}) known to originate from sea spray and soil. On the other hand, the absence of fine mode for NO_3^- could result from adsorption of HNO_3 on sea-salt particles. HNO_3 can further react with sea salt resulting in a chloride deficit via formation of gaseous HCl following the reaction:

$$HNO_{3(gas)} + NaCl \rightarrow NaNO_3 + HCl_{(gas)}.$$
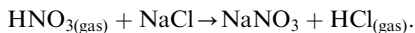
To check this possibility Fig. 4 presents the variation of sodium in excess, relative to chloride, as a function of NO_3^- concentrations. The statistically significant corre-

lation ($r^2 = 0.73$; $P<0.05$) with a slope of 0.80 indicates that this reaction can account for the majority of nitrate levels observed during the experiment. In a recent study performed in the western Mediterranean, Sellegri et al. (2001) showed the presence of NO_3^- also in the fine mode 100–200 km offshore. This pattern was observed only when the air masses originated from Western Europe and was attributed to the formation of NH_4NO_3, probably reflecting the more important contribution of NH_3 sources to the western basin compared to the eastern one. Other studies in the Mediterranean have also observed a high marine borne NO_3^- component in the aerosol mass (Eleftheriadis et al., 1998) and the absence of fine nitrate to the expense of coarse nitrate during summer (Eleftheriadis et al., 1999).

MS^-, presents the same type of distribution as SO_4^{2-}, with a small maximum in the coarse mode and the main maximum in the accumulation mode indicating formation via absorption on coarse particles and gas-to-particle conversion (Fig. 3c), respectively. Note, however, that the MS^-/nss-SO_4^{2-} ratio presents higher values in the coarse mode (by a factor of 2–3) compared to the fine fraction probably due to the lower vapor pressure of MSA compared to H_2SO_4.

Although all the carboxylic, dicarboxylic and ketoacids studied in this work are distributed mainly in the fine mode, they present significant differences in their size distribution as depicted in (Figs. 3d–h).

Thus oxalate and the other dicarboxylic acids present a bi-modal distribution with a clear maximum in the fine mode (<1 μm) and a second smaller in the coarse mode (>1 μm) since more than 65% of their mass is found in the fine mode. Note also that a small part of the dicarboxylic anions (about 5–10%) but comparable to that of nss-SO_4^{2-} and NH_4^+ is found in the Aitken mode (<0.1 μm) in agreement with the earlier works (Matsumoto et al., 1998; Kerminen et al., 1999) indicating the potential role of dicarboxylic acids as CCN.

Although carboxylic acids are also mainly distributed in the fine mode, no clear pattern is found in agreement with Matsumoto et al. (1998). Note that during this campaign acetic and formic acids have been measured in the gas phase at levels significantly higher than in the aerosol phase (by a factor of 5–10). This is due to the fact that both acetic and formic acids have high vapor pressure and thus the aerosol phase corresponds to a very small fraction for the above acids.

Finally, although pyruvate is mainly distributed in the fine mode during summer (more than 85%), it presents a non-negligible coarse fraction during winter (data not shown). The decrease in the ambient temperature and/or source strength could account for such distribution. Indeed, it has been proposed that pyruvic acid has also a marine origin via the photo-oxidation of biogenic compounds emitted from seawater (Kawamura and Sakaguchi, 1999). Thus, lower productivity and lower
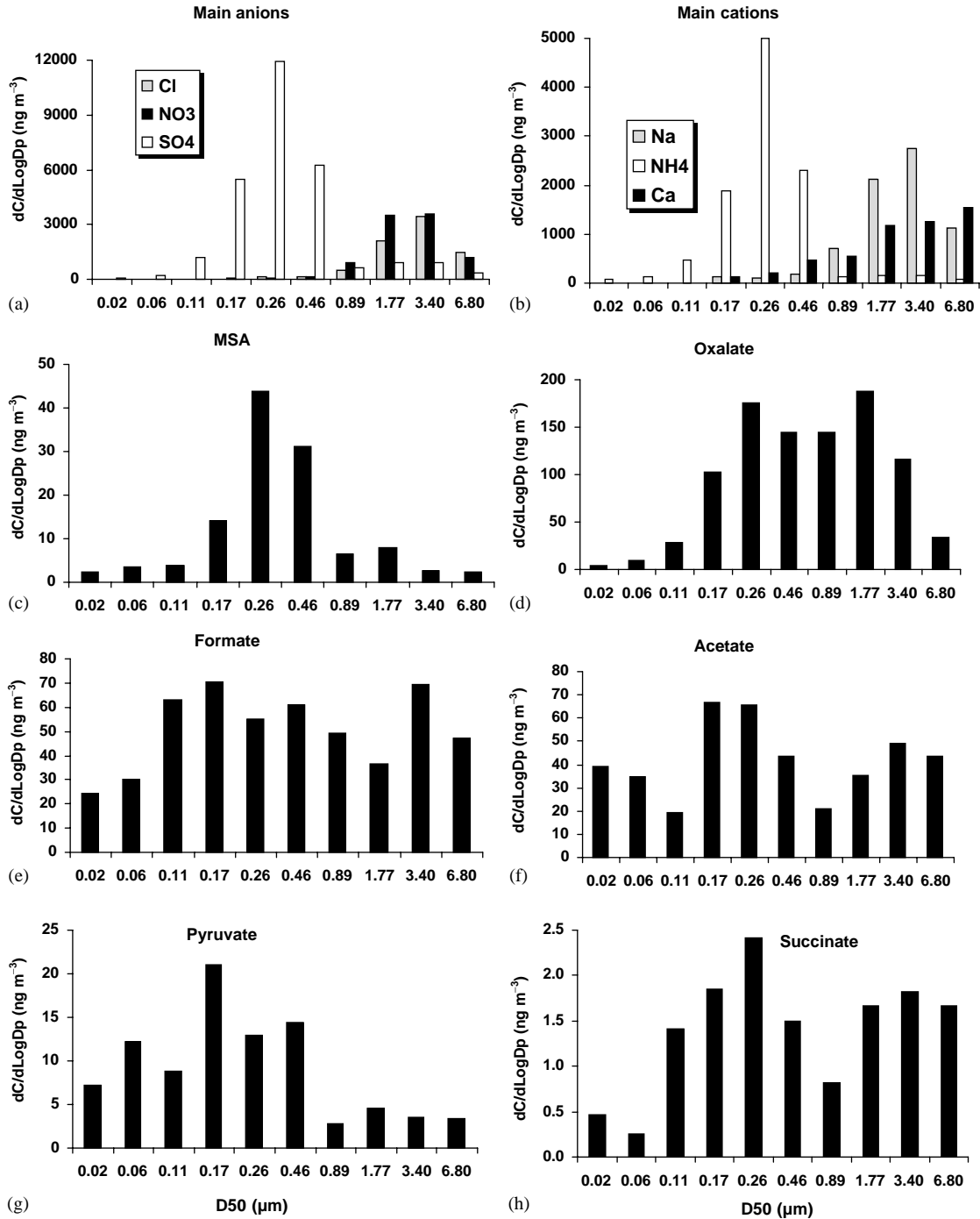
Fig. 3. Particle size distribution of the main anions (a), cations (b), MS⁻(c), oxalate (d), formate (e), acetate (f), pyruvate (g) and succinate (h) during the summer campaign.

photochemistry could account for a decrease in the strength of the biogenic source of pyruvic acid during winter.

Of particular interest is whether air mass origin can influence the size distribution of the examined ions or if a seasonal trend in their size distribution exists.

Figs. 5a–d show the size distribution of MS^- and $C_2O_4^{2-}$ as a function of season (summer, winter) and air-mass origin (only during summer when sufficient samples exist). For MS^- as for all the main anions and cations no significant change in the size distribution is observed as a function of season. On the other hand for $C_2O_4^{2-}$, a clear decrease in the maximum value in the accumulation mode is observed probably reflecting, change in gas-to-particle distribution due to lower temperature encountered during winter and/or decrease in the source strength as in the case of pyruvate. Regarding the sector influence a clear change is observed for both MS^- and

$C_2O_4^{2-}$ under west sector (pure marine) influence compared to the N/NE sector (anthropogenic influence). For both species a relative increase in the coarse mode fraction occurred and result from adsorption of the gaseous precursors of oxalate (oxalic acid) and MS^- (MSA and/or dimethylsulfoxide) on alkaline medium such as sea spray. Additional decrease in the contribution of fine particles from long-distance transport from continental sources cannot be ruled out for oxalate under marine influence, in agreement with the observations of Matsumoto et al. (1998).

Figs. 6a and b present the variation of the sum of cations and anions as a function of aerosol diameter for both seasons. During winter (Fig. 6b) with the exception of a small cation deficit observed in the accumulation mode at 270 nm the sum of anions matches very well the sum of cations indicating complete neutralization of the aerosols. The deficit at the accumulation mode is due to H^+ since NH_4^+ levels were not sufficient enough to neutralize the nss-SO_4^{2-} levels (NH_4^+/nss-SO_4^{2-} molar ratio of 1.9). On the other hand, during summer (Fig. 6a) and when the samples collected under local influence are excluded (wind speed $<2\,\mathrm{m\,s^{-1}}$), in addition to the deficit in the fine mode a clear deficit in the coarse mode is also observed. The deficit in the accumulation mode results (as for the winter samples) from the partial neutralization of NH_4^+ from nss-SO_4^{2-} (NH_4^+/nss-SO_4^{2-} molar ratio of 1.5), whereas the deficit

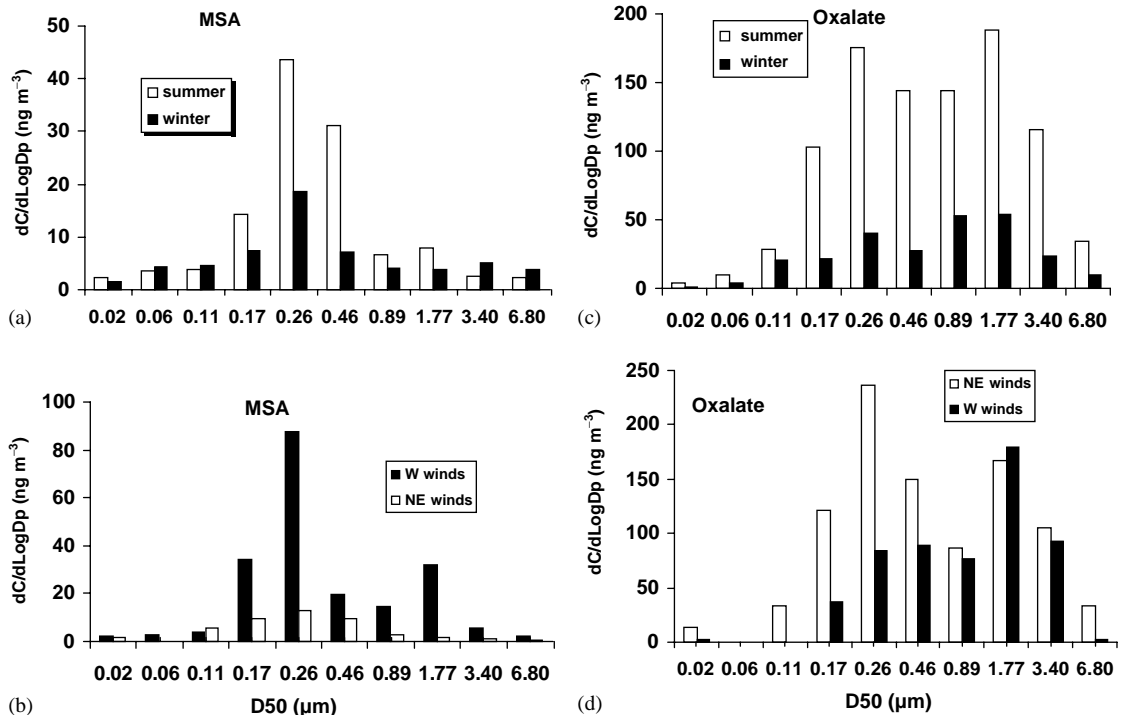Fig. 4. Variation of sodium in excess versus NO_3^- concentrations measured during the experiment.

Fig. 5. Size distribution of MS^- (a) and $C_2O_4^{2-}$ (b) as a function of season and air mass origin.
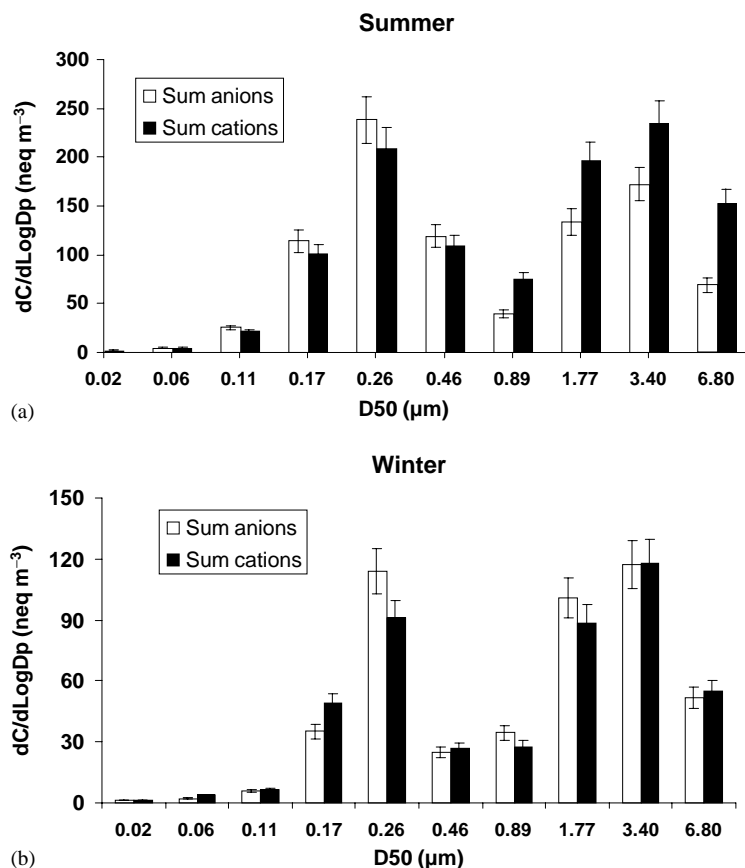
Fig. 6. Variation of sum of cations and anions as a function of aerosol diameter for both summer (a) and winter (b). Error bars correspond to the total error in the ionic species measurements and are estimated to be of the order of 10–15% for the sum of anions and cations, respectively.

in the coarse mode could be due to CO_3^{2-} (Mihalopoulos et al., 1997). If this is the case, CO_3^{2-} are expected to associate with Ca^{2+}. To check this possibility, Fig. 7 presents the variation of anions deficit (sum of stages 7–10) versus the Ca^{2+} concentrations. The statistically significant correlation ($r^2 = 0.96$; $P < 0.05$) with slope close to unity (1.11), indicates that the anions deficit is most probably due to carbonates associated with Ca^{2+}.

3.1.5. Contribution of ionic mass to the total mass

Figs. 8a and b present the sum of ionic mass (IM) and the aerosol mass (weight) measured during this experiment as a function of aerosol diameter for both seasons. During summer, carbonate mass is also taken into consideration in the ionic mass, assuming a molar ratio of unity relative to Ca^{2+} as deduced from Fig. 7. Aerosol mass ranged from 35.7 μg m^{-3} during summer to 15.4 μg m^{-3} during winter and presents two well distinguished maxima: one in the fine mode and the other in the coarse mode with a coarse/fine ratio ranging from 1.2 during summer to 1.5 during winter. The

aerosol mass measured during both seasons is in good agreement with the values reported for European rural areas (Lazaridis et al., 2001 and references therein).

Ionic mass follows quite well the total aerosol mass and accounts for about 56% and 58% of the mass determined during winter and summer respectively. No significant variation exists between the relative contribution of ionic mass to the corresponding total mass for both the coarse and fine fraction. The contribution of ionic mass to the total mass agrees quite well with the figures reported for rural areas in Europe (Zappoli et al., 1999).

Figs. 9a and b report the relative contribution of the main ionic and organic ions respectively. SO_4^{2-} is the main ion in the fine mode accounting for about 65% of the total ionic mass in agreement with the results reported by Sellegri et al. (2001). Together with NH_4^+ with which it is associated, they account for up to 90% of the total mass in the fine fraction. On the other hand, in the coarse mode there is no prevailing ion since five ions (Na^+, Cl^-, Ca^{2+}, CO_3^{2-} and NO_3^-) have almost
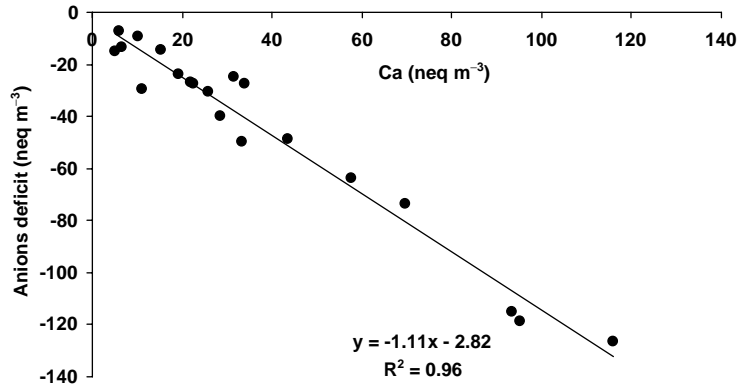
Fig. 7. Variation of anions deficit (sum of stages 7–10) versus the Ca^{2+} concentrations during the summer campaign.
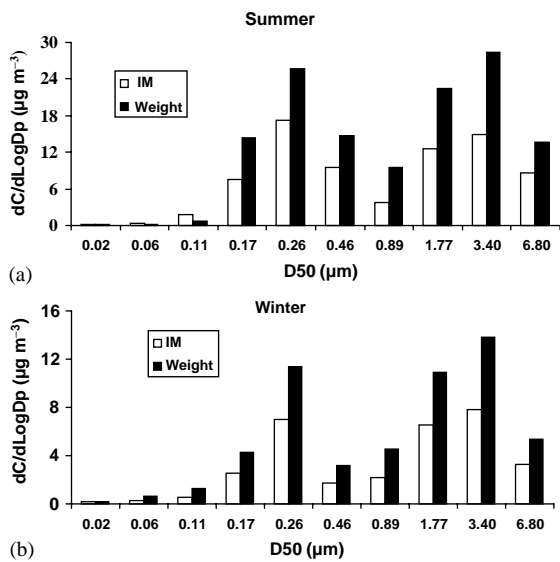

Fig. 8. Sum of the mean ionic mass (IM) measured during this experiment as a function of aerosol diameter and for summer (a) and winter (b). For comparison, the mean aerosol mass (weight) determined for each stage and for each season is also reported.

equal participation and account for up to 90% of the total ionic mass in the coarse fraction.

The situation is more uniform for the organic ions (Fig. 9b). Oxalate is found to be the main ionic specie both in the coarse and fine modes. Together with acetate and formate they can account for up to 90% of the total organic ionic mass. During the summer campaign when acetate and formate are measured, the total mass of measured organic ions is estimated to be 0.58 μg m^{-3}. Thus, although they account for only up to 1–2% of the total mass fraction, they can account for up to 15% of the total organic carbon mass estimated to be of the

order of 3.8 μg m^{-3} (discussed in detail in the following paragraph).

3.1.6. Mass closure

During all campaigns the impactor samples were analyzed by particle-induced X-ray emission (PIXE) for Al, Si, K, Ca, Ti, Mn, Fe, Sr, S, Cl, Ni, V, Cu, Cr, Zn, and Pb. Analyses were performed on a 3 MeV Van de Graaff electrostatic accelerator at the Nuclear Physics Institute in Řež in Prague. Two proton beam energies of 1.31 and 2.35 MeV were used to irradiate samples. More details on these measurements will be presented elsewhere (Smolik et al., unpublished data). Dust concentration is derived either from the Al, Fe or Si mass and by assuming a ratio relative to dust of 7.7%, 5% and 30% for Al, Fe and Si, respectively (Wedepohl, 1995). Using this procedure, dust was determined both for coarse and fine fractions using the three diagnostic ratios and was found to be 0.90 and 5.77 μg m^{-3} during winter and summer, respectively. The standard deviation of the mean of the dust determinations using the three diagnostic ratios was of the order of 10–30% for the fine and the coarse mode, respectively.

Additional analysis for both elemental (EC) and organic carbon (OC) has been performed on eight (8), 47 mm quartz fiber filters collected during both seasons using the thermo-optical determination technique and an instrument from Sunset Laboratory Inc. (Birch and Cary, 1996; NIOSH method 5040). Although their concentrations range from 0.09–0.68 and 0.28–2.23 μg m^{-3} for EC and OC, respectively, their ratio (EC/OC) was relatively constant with an average value of 0.3 throughout both seasons. The concentration of particulate organic matter (POM) was determined by multiplying the OC concentration by 1.7, which is the average ratio of the mass of carbon-containing species to carbon mass assumed to be distributed between fine and
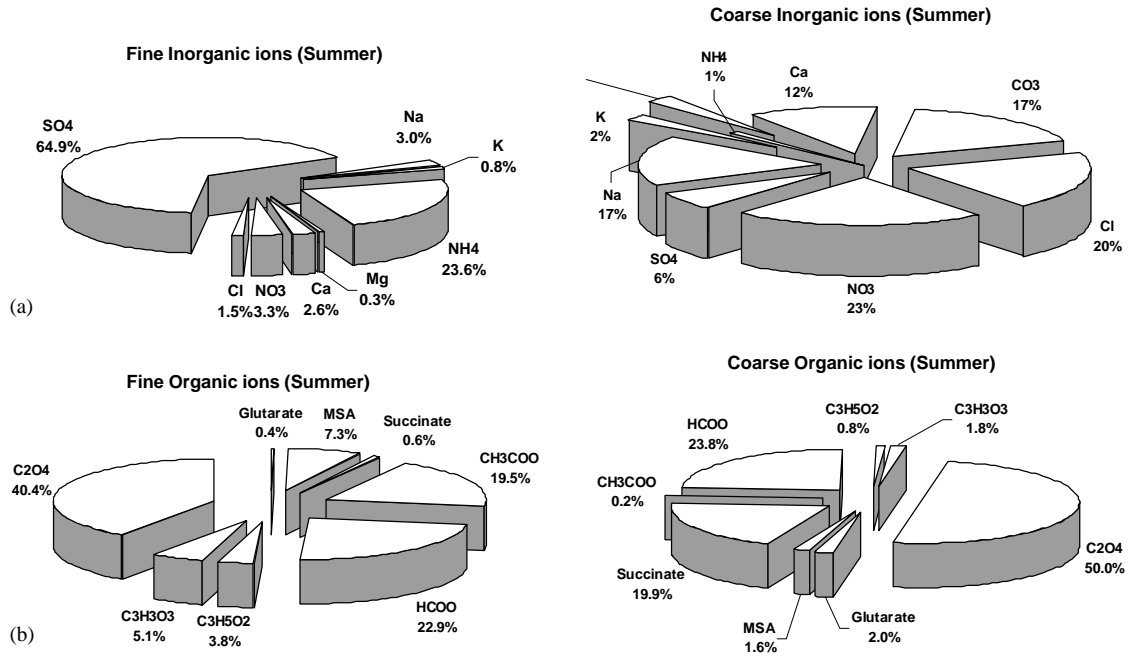
Fig. 9. Relative contribution of the main ionic (a) and organic ions (b) for both modes during the summer campaign.
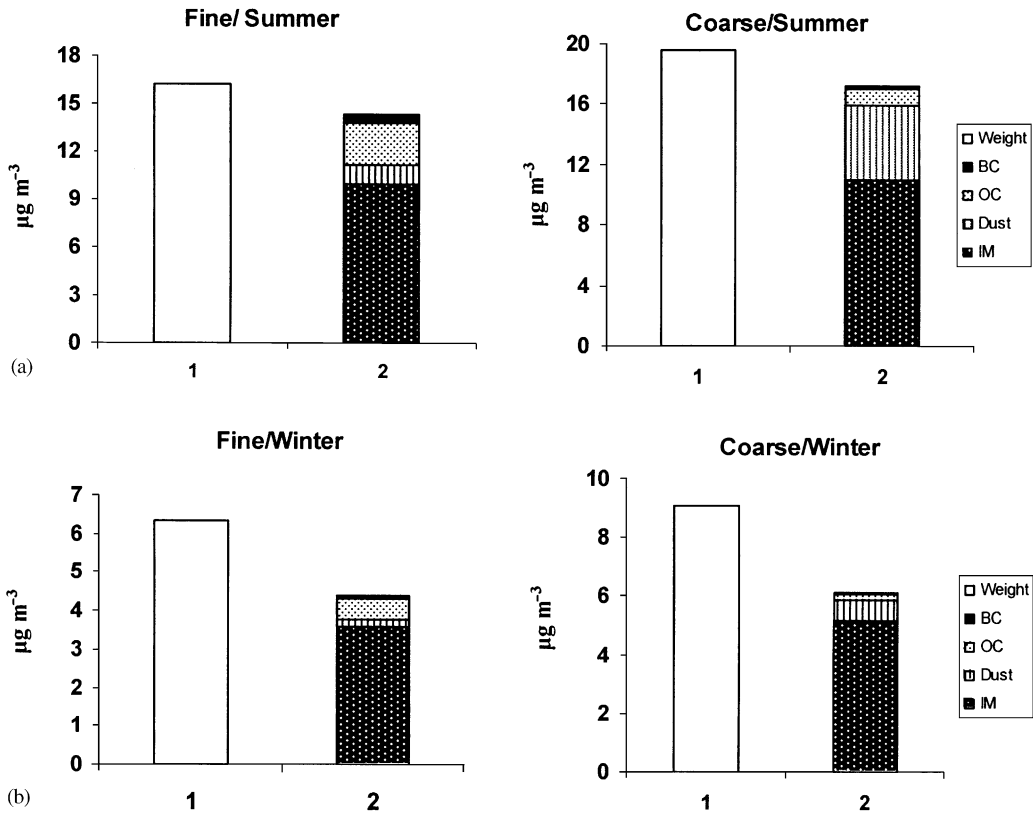

Fig. 10. Mass closure based on a comparison between the measured mass on the one hand and the measured total ionic mass, dust, EC and POM masses for both coarse (> 1 μm) and fine (< 1 μm) fractions and for both summer (a) and winter campaigns (b), respectively.

coarse mode with a ratio of 7/3 (Quinn et al., 2000; Putaud et al., 2000; Neusüß et al., 2000). During summer the amount of analyzed filters for EC/OC (8) was lower than the IC filters (22). To extrapolate the EC/OC observations for the whole period the measured mean EC value obtained using the thermo-optical determination technique ($0.44\ \mu g\ m^{-3}$) has been compared with the corresponding mean value ($0.52\ \mu g\ m^{-3}$) determined using a particle soot absorption particle (PSAP) apparatus operating during the whole campaign with a sampling step of 5 min ($r^2 = 0.71$ between the two data sets when one value is excluded with a short common sampling time). Thus, based on the determined EC/OC ratio and the measured EC levels during the whole campaign using the PSAP (mean value of 0.66), mean OC concentrations during the campaign have been derived.

A mass closure based on a comparison between the measured mass and the measured total ionic, dust, EC and POM masses was thus attempted. Figs. 10a and b report the results of such comparison for both summer and winter campaigns and for both coarse and fine fractions. In the fine fraction SO_4^{2-} and OC are the two main constituents since they account for up to 38% and 16%, respectively. On the other hand, no major constituent in the coarse mode was found. The agreement between the measured and estimated mass is quite reasonable during summer (estimated mass was about 12% lower than the measured, Fig. 10a and b). On the other hand, the discrepancy between measured and calculated mass was higher during winter (up to 30%). Water and the uncertainty in the use of diagnostic ratios for the dust determination (Andreae et al., 2002) can account for part of the missing compounds.

4. Conclusions

Determination of the chemical composition of aerosols has been performed in 30 size-resolved atmospheric aerosol samples collected with a Berner low-pressure impactor during two campaigns conducted at a coastal site in the Eastern Mediterranean in the frame of the EU funded SUB-AERO project in July 2000 and in January 2001.

- Although organic ions account for only up to 1–2% of the total mass fraction, they can contribute up to 15% of the total organic carbon mass (at least during summer when all the main organic ionic species were measured). Oxalate is found to be the main ionic specie both in the coarse and in the fine mode. During summer oxalate, acetate and formate all together can account for up to 90% of the total organic ionic mass.

- During both seasons sulfate was found to be the main ion in the fine mode accounting for about 65% of the total ionic mass. Together with NH_4^+ they account for up to 90% of the total ionic mass in the fine fraction. In the coarse mode there is no prevailing ion since the five ions Na^+, Cl^-, Ca^{2+}, CO_3^{2-} and NO_3^- have almost equal participation and account for up to 90% of the total ionic mass.

- A clear deficit has been observed for chloride, which could result from adsorption of HNO_3 on sea-salt particles. HNO_3 can further react with sea salt resulting in a chloride deficit via formation of gaseous HCl. The statistically significant correlation ($r^2 = 0.73$; $P < 0.05$) between sodium in excess and NO_3^- concentrations with a slope of 0.8, indicates that this reaction can account for the majority of the nitrate observed during the experiment.

- Mass closure was attended on the basis of a comparison between the measured mass and the measured total ionic mass, dust, EC and POM masses. The agreement between the measured and estimated masses is quite good during summer (discrepancy $< 12\%$). On the other hand, the discrepancy between measured and calculated masses during winter is larger (around 30%). Water can account for part of the missing compounds especially in the coarse mode.

References

Andreae, M.O., Talbot, R.W., Li, S.M., 1987. Atmospheric measurements of pyruvic and formic acid. Journal of Geophysical Research 92, 6635–6641.

Andreae, T.W., Andreae, M.O., Ichoku, C., Andreae, Maenhaut, W., Cafmeyer, J., Karnieli, A., Orlovsly, L., 2002. Light scattering by dust and anthropogenic aerosol at a remote site in the Negev desert, Israel. Journal of Geophysical Research 107, 252–290.

Baboukas, E.D., Kanakidou, M., Mihalopoulos, N., 2000. Carboxylic acids in gas and particulate phase above the Atlantic ocean. Journal of Geophysical Research 105, 14459–14471.

Birch, M.E., Cary, R.A, 1996. Elemental carbon-based method for monitoring occupational exposures to particulate diesel exhaust. Aerosol Science and Technology 23 (3), 221–241.

Charlson, R.J., Langner, J., Rodhe, H., Leovy, C.B., Warren, S.G., 1991. Perturbation of the northern hemisphere radiative balance by backscattering from anthropogenic sulfate aerosols. Tellus 43AB, 152–163.

Chebbi, A., Carlier, P., 1996. Carboxylic acids in the troposphere, occurrence, sources and sinks: a review. Atmospheric Environment 30, 4233–4249.

Draxler, R.R., Hess, G.D., 1998. An overview of the HYSPLIT_4 modelling system for trajectories, dispersion and deposition. Australian Meteorological Magazine 47, 295–308.

Eleftheriadis, K., Balis, D., Ziomas, I., Colbeck, I., Manalis, N., 1998. Atmospheric aerosol and gaseous species in Athens, Greece. Atmospheric Environment 32 (12), 2183–2191.

Eleftheriadis, K., Meng-chen Chung, Michaleas, S., Colbeck, I., 1999. Atmospheric aerosol evolution and transport over Athens. In: Th. Lekkas (Ed.), Proceedings of the Sixth Conference on Environmental Science and Technology, 30th August–2nd September 1999, Samos, Greece, Vol. A'. University of the Aegean, pp. 137–144.

Ganor, E., Mamane, Y., 1982. Transport of Saharan dust across the Eastern Mediterranean. Atmospheric Environment 16, 581–587.

Hillamo, R.E., Kaupinnen, E.I., 1991. On the performance of the Berner low pressure impactor. Aerosol Science and Technology 14, 33–47.

Ichoku, C., Andreae, M.O., Andreae, T.W., Meixner, F.X., Schebeske, G., Formenti, P., Maenhaut, W., Cafmeyer, J., Ptasinski, J., Karnieli, A., Orlovsly, L., 1999. Interrelationships between aerosol characteristics and light scattering during late winter in an Eastern Mediterranean arid environment. Journal of Geophysical Research 104, 24371–24393.

IPCC, 2001. Climate change 2001. In: Watson, R., et al. (Eds.), The Scientific Basis. Summary for Policy Makers and Technical Summary of the Working Group 1 Report. Cambridge University Press, Cambridge, 98p.

Jaffrezo, J.-L., Calais, N., Bouchet, M., 1998. Carboxylic acids measurements with ion chromatography. Atmospheric Environment 32, 2705–2708.

Kawamura, K., Sakaguchi, F., 1999. Molecular distributions of water soluble dicarboxylic acids in marine aerosols over the Pacific Ocean including tropics. Journal of Geophysical Research 104, 3501–3509.

Kawamura, K., Usukura, K., 1993. Distributions of low molecular weight dicarboxylic acids in the northern Pacific aerosol samples. Journal of Oceanography 49, 271–283.

Kawamura, K., Kasukabe, H., Barrie, L., 1996. Source and reaction pathways of dicarboxylic acids, ketoacids and dicarbonyls in Arctic aerosols: one year of observations. Atmospheric Environment 30, 1709–1722.

Kerminen, V.-M., Teinila, K., Hillamo, R., Makela, T., 1999. Size-segregated chemistry of particulate dicarboxylic acids in the Arctic atmosphere. Atmospheric Environment 33, 2089–2100.

Khare, P., Kumar, N., Satsangi, G.S., Kumari, K.M., Srivastava, S.S., 1998. Formate, acetate in particulate matter and dust fall at Dayalbagh, Agra, India. Chemosphere 36, 2993–3002.

Kouvarakis, G., Mihalopoulos, N., 2002. Seasonal variation of gaseous dimethylsulfide and sulfur species in aerosol phase in the Eastern Mediterranean atmosphere. Atmospheric Environment 36, 929–938.

Kouvarakis, G., Tsigaridis, K., Kanakidou, M., Mihalopoulos, N., 2000. Temporal variations of surface regional background ozone over Crete Island in southeast Mediterranean. Journal of Geophysical Research 105, 4399–4407.

Kubilay, N., Nickovic, S., Moulin, C., Dulac, F., 2000. An illustration of the transport and deposition of mineral dust onto the eastern Mediterranean. Atmospheric Environment 34, 1293–1303.

Krivácsy, Z., Hoffer, A., Sárvári, Zs., Temesi, D., Baltensperger, U., Nyeki, S., Weingartner, E., Kleefeld, S., Jennings, S.G., 2001. Role of organic and black carbon in the chemical composition of atmospheric aerosol at European background sites. Atmospheric Environment 35, 6231–6244.

Lazaridis, M., Gehring, R., Torseth, K., Yttri, K.E., Semb, A., Larssen, S., Stordal, F., Schaug, J., Hov, O., Hjellbrekke, A., Hanssen, J., Dye, C., Huglin, C., Hofer, P., Smolik, J., Zdimal, V., Eleftheriadis, K., Colbeck, I., Nyeki, S., Mihalopoulos, N., Harnvanek, V., 2001. Status Report with Respect to Measurements of Particulate Matter in EMEP. EMEP/CCC-report 5/2001, O-98134, August 2001, 85pp.

Li, S.M., Winchester, J.W., 1989. Geochemistry of organic and inorganic ions of a late winter Arctic aerosols. Atmospheric Environment 23, 2401–2415.

Matsumoto, K., Tanaka, H., Nagao, I., Ishizaka, Y., 1997. Contribution of particulate sulfate and organic carbon to cloud condensation nuclei in the marine atmosphere. Journal of Geophysical Research 24, 655–658.

Matsumoto, K., Nagao, I., Tanaka, H., Miyaji, H., Iida, T., Ikebe, Y., 1998. Seasonal characteristics of organic and inorganic species and their size distributions in atmospheric aerosols over the northwest Pacific Ocean. Atmospheric Environment 32, 1931–1946.

Mihalopoulos, N., Stephanou, E., Kanakidou, M., Pilitsidis, S., Bousquet, P., 1997. Tropospheric aerosol ionic composition above the Eastern Mediterranean Area. Tellus B 49B, 314–326.

Moulin, C., Dulac, F., Lambert, C.E., Chazette, P., Chatenet, B., Lavenu, F., 1997a. Long-term daily monitoring of Saharan dust load over ocean using Meteosat ISCCP-B2 data, 2, Accuracy of the model and validation using Sun photometer measurements. Journal of Geophysical Research 102, 16959–16969.

Moulin, C., Guillard, F., Dulac, F., Lambert, C.E., 1997b. Long-term daily monitoring of Saharan dust load over ocean using Meteosat ISCCP-B2 data, 1, Methodology and preliminary results for 1983–1994 in the Mediterranean. Journal of Geophysical Research 102, 16947–16958.

Neusüß, C., Pelzing, M., Plewka, A., Hermann, H., 2000. A new analytical approach for size-resolved speciation of organic compounds in atmospheric aerosols particles: methods and first results. Journal of Geophysical Research 105, 4513–4527.

Polian, G., Lambert, G., Ardouin, B., Jégou, A., 1986. Long range transport of continental radon in Subantarctic areas. Tellus 38B, 178–189.

Putaud, J.-P., Van Dingenen, R., Magnoni, M., Virkkula, A., Maring, H., Prospero, J.M., Swietlicki, E., Berg, O.H., Hillamo, R., Makela, T., 2000. Chemical mass closure and assessment of the origin of the submicron aerosol in the marine boundary layer and the free troposphere at Tenerife during ACE. Tellus 52B, 141–168.

Quinn, P.K., Bates, T.S., Coffman, D.J., Miler, T.L., Johnson, J.E., Covert, D.S., Putaud, J.P., Neusüß, C., Novakov, T., 2000. A comparison of aerosols chemical and optical properties from the first and the second aerosol characterization experiment. Tellus 52B, 239–257.

Sellegri, K., Gourdeau, J., Putaud, J.P., Despiau, S., 2001. Chemical composition of marine aerosol in a Mediterranean coastal zone during the FETCH experiment. Journal of Geophysical Research 106, 12023–12037.

Wedepohl, K.H., 1995. The composition of the continental crust. Geochimica et Cosmochimica Acta 59, 1217–1232.

Yu, S., 2000. Role of organic acids (formic, acetic, pyruvic and oxalic) in the formation of cloud condensation nuclei (CCN): a review. Atmospheric Research 53, 185–217.

Zappoli, S., Andracchio, A., Fuzzi, S., Facchini, M.C., Gelencser, A., Kiss, Gy., Krivacsy, Z., Molnar, A., Meszaros, E., Hansson, H.-C., Rosman, K., Zebuhr, Y., 1999. Inorganic, organic and macromolecular components of fine aerosols in different areas of Europe in relation to their water solubility. Atmospheric Environment 33, 2733–2743.